Comparative Study of UAV Mapping with and without Ground Control Points (GCPs)

Thammaboribal, P.,[1*] Tripathi, N. K.[1] and Lipiloet, S.[2]
[1]Asian Institute of Technology, School of Engineering and Technology, P. O. Box 4, Klong Luang, Pathumthani 12120, Thailand, E-mail: prapasgnss@gmail.com
[2]Department of Civil Engineering, Faculty of Engineering, Rajamangala University of Technology Thanyaburi, Pathumthani 12120, Thailand
**Corresponding Author*

DOI: https://doi.org/10.52939/ijg.v22i3.4861

Abstract
Unmanned Aerial Vehicles (UAVs) have transformed geospatial data acquisition, yet the necessity of Ground Control Points (GCPs) for spatial accuracy versus operational efficiency remains a critical topic of investigation. This study presents a comparative analysis of UAV mapping accuracies achieved with and without the integration of GCPs. Conducted at the Asian Institute of Technology (AIT) in Pathum Thani, Thailand, the research utilized a DJI Phantom 4 Pro for aerial imagery and a Javad TRIUMPH-2 GNSS receiver to establish survey-grade GCPs and Check Points (CPs) via Real-Time Kinematic (RTK) methods. Flight parameters included a 90-meter altitude with 70% forward and side overlap, yielding a Ground Sampling Distance (GSD) of 3.45 cm/pixel across a 0.252 km² area. The photogrammetric processing resulted in a Root Mean Square Error (RMSE) of 26.26 cm for GCPs and 76.76 cm for independent CPs. The findings indicate that while orthophotos and Digital Surface Models (DSMs) processed without GCPs exhibit smoother visual aesthetics and slightly more visible detail, they suffer from significant systematic vertical errors, such as the "doming" effect, and lack absolute geospatial accuracy. Conversely, GCP-constrained models achieve much higher absolute positional accuracy but reveal geometric distortions around vertical structures as the software forces the imagery to match precise ground coordinates. Ultimately, GCPs are essential for mapping projects requiring rigorous absolute accuracy, whereas unconstrained workflows may suffice for relative topographic visualization.

Keywords: Georeferencing Accuracy, Ground Control Points, Orthophoto, Structure-From-Motion, UAV Photogrammetry

1. Introduction

Unmanned Aerial Vehicles (UAVs) have emerged as a transformative technology in the field of geospatial data acquisition [1][2] and [3], 3D mapping [4], tree height measurement [5] , coastal mapping [6], and volume determination [7][8] and [9], offering a flexible, cost-effective, and high-resolution alternative to traditional airborne and terrestrial surveying methods [10] and [11]. Advances in onboard Global Navigation Satellite Systems (GNSS), inertial measurement units (IMUs), and photogrammetric processing software have significantly improved the accuracy and efficiency of UAV-based mapping workflows [12]. In particular, Structure-from-Motion (SfM) and multi-view stereo (MVS) techniques, as implemented in widely used platforms such as Agisoft Metashape and Pix4Dmapper, have enabled the generation of dense point clouds, digital surface models (DSMs), digital terrain models (DTMs), and orthomosaics from overlapping aerial imagery [13]. These developments have expanded the applicability of UAV mapping across disciplines including civil engineering [14], surveying [15], urban planning [16] and [17], archelogy [18], environmental monitoring [19] and [20], precision agriculture [21], and disaster management [22][23] and [24].

A critical factor influencing the positional accuracy of UAV-derived products is the georeferencing strategy employed during data acquisition and processing. Traditionally, Ground Control Points (GCPs) well-distributed, precisely surveyed reference points on the ground surface have been used to constrain photogrammetric models and improve both horizontal and vertical accuracy [25].

GCPs are typically measured using high-precision surveying techniques such as Real-Time Kinematic (RTK) or Post-Processed Kinematic (PPK) GNSS. While the incorporation of GCPs can substantially enhance geospatial accuracy, it also introduces additional time, labor, and logistical requirements, particularly in remote, hazardous, or large-scale study areas.

Recent advancements in UAV platforms equipped with onboard RTK/PPK GNSS receivers have enabled direct georeferencing approaches, reducing or potentially eliminating the need for extensive ground control [26]. Systems such as the DJI Phantom 4 RTK and senseFly eBee X provide centimeter-level positioning accuracy by integrating high-precision GNSS data with image acquisition [27] . These technologies promise streamlined field operations and reduced project costs. However, the extent to which direct georeferencing can reliably substitute or minimize the use of GCPs remains an area of active investigation, particularly in applications requiring rigorous vertical accuracy or compliance with mapping standards [28] and [29].

While GCPs are widely considered the gold standard for achieving centimeter-level absolute accuracy [30], their implementation introduces significant operational bottlenecks. The planning, physical distribution, and measurement of GCPs are highly labor-intensive and time-consuming processes. In many surveying projects, the field data collection for GCPs can account for a substantial majority of the total project time and budget [31]. Furthermore, in hazardous, heavily vegetated, or geographically inaccessible terrains (e.g., steep slopes, marshlands, or post-disaster zones), establishing a robust network of GCPs is often impractical or entirely impossible. To circumvent the limitations associated with GCPs, the geospatial industry has seen a rapid adoption of Direct Georeferencing (DG) techniques, facilitated by equipping UAVs with onboard Real-Time Kinematic (RTK) or Post-Processed Kinematic (PPK) GNSS receivers [32]. These systems accurately record the precise spatial coordinates of the camera's optical center at the exact moment of each image capture. Theoretically, RTK/PPK-enabled UAVs can drastically reduce, or even eliminate, the dependency on GCPs while maintaining survey-grade accuracy. However, reliance on direct georeferencing introduces its own set of variables, such as the accuracy of lever-arm offsets, synchronization errors between the camera and GNSS receiver [33], and the dependency on a continuous connection to a base station or Continuously Operating Reference Station (CORS) network [34].

Although manufacturers often claim that RTK/PPK systems eliminate the need for GCPs, empirical studies suggest that the reality is more nuanced, particularly concerning vertical accuracy (Z-axis) and lens calibration stability. There remains a critical need to rigorously evaluate the trade-offs between time, cost, and spatial accuracy across different georeferencing methodologies [35] and [36]. Therefore, this study presents a comparative analysis of UAV mapping accuracies achieved with and without the integration of GCPs. The primary objectives of this research are to conduct a comprehensive comparative assessment of UAV-based mapping performed with and without Ground Control Points. By evaluating horizontal and vertical positional accuracy, this research seeks to determine the practical trade-offs between traditional GCP-supported workflows and direct georeferencing approaches. The findings are intended to provide evidence-based recommendations for practitioners and researchers regarding optimal georeferencing strategies in different surveying contexts.

2. Methodology

2.1 Study Area

The research was conducted at the main campus of the Asian Institute of Technology (AIT), located in the Khlong Luang district of Pathum Thani province, Thailand (approximately 40 kilometers north of central Bangkok) (Figure 1). Situated within the lower Chao Phraya River basin, the site represents a characteristic peri-urban environment in a tropical climate. The selection of the AIT campus is highly strategic for this specific comparative study. As a self-contained, institutional environment, it provides the secure, controlled access required for extensive field operations. This logistical advantage allowed for the undisturbed establishment and measurement of a high-density, survey-grade GCP network using terrestrial GNSS rovers. This extensive physical network is critical for establishing the absolute "ground truth" necessary to cross-validate the spatial accuracies of the subsequent un-controlled (no-GCP) RTK/PPK flight data. Consequently, the diverse, micro-urban landscape of the AIT campus provides a robust, real-world testing ground that closely mirrors the complexities encountered in professional commercial surveying.

2.2 Instrument Used

2.2.1 DJI Phantom 4 pro

The DJI Phantom 4 Pro (Figure 2) was selected as the primary aerial data acquisition instrument for this study due to its proven reliability, high-resolution imaging capability, and widespread adoption in professional photogrammetric applications.

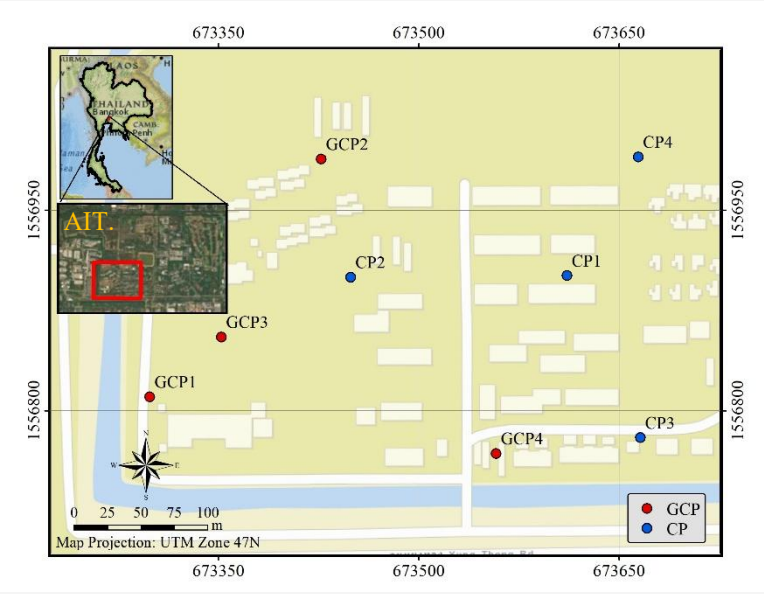

Figure 1: Test site in Asian Institute of Technology (AIT), Pathumthani, Thailand

Figure 2: DJI Phantom 4 Pro

As a multirotor unmanned aerial vehicle (UAV) platform designed for mapping and surveying tasks, the Phantom 4 Pro integrates advanced flight stability systems, precise navigation sensors, and a high-performance onboard camera, making it well suited for comparative analysis of UAV mapping workflows conducted with and without Ground Control Points (GCPs).

Phantom 4 Pro is equipped with multi-constellation GNSS support (GPS and GLONASS), enabling accurate geotagging of captured imagery. Although the standard Phantom 4 Pro does not include onboard RTK positioning, its GNSS-based image metadata provides sufficient positional information for indirect georeferencing workflows and for comparison with GCP-supported processing. This capability makes it particularly appropriate for a study aimed at evaluating differences between mapping results generated with ground control and those relying solely on onboard positioning data [37]. Furthermore, the exterior orientation (camera position and attitude) recorded at the moment of image capture contains this meter-level ambiguity, the un-constrained photogrammetric block (the "without GCPs" scenario) relies entirely on relative image matching [38]. This inherently leads to systematic error propagation, global datum shifts, and non-linear deformations such as the aforementioned topographic "doming" effect. Consequently, the UAV provides an optimal, highly sensitive mechanism for this research: it allows for a stark, mathematically rigorous quantification of the absolute error inherent in uncontrolled SfM workflows, establishing a clear baseline against which the corrective power of a high-density GCP network can be measured.

The Phantom 4 Pro's flight time of approximately 25–30 minutes per battery cycle supports efficient coverage of medium-sized study areas while maintaining high image overlap requirements for photogrammetric reconstruction [39]. Its integrated obstacle sensing system enhances operational safety, which is particularly valuable when flying over mixed land-cover environments such as built-up areas, vegetation, and open fields.

The selection of the DJI Phantom 4 Pro also reflects its extensive validation in academic and professional literature, where it has been widely used for topographic mapping, infrastructure inspection, environmental monitoring, and volumetric analysis. Its balance between cost, performance, and data quality makes it representative of commonly deployed UAV systems in engineering and geospatial practice. Consequently, findings derived from this research can be generalized to similar multirotor UAV platforms used in mapping applications.

2.2.2 GNSS receiver

The Javad TRIUMPH-2 (Figure 3) was employed in this study as the primary ground-based positioning instrument for establishing Ground Control Points (GCPs) and independent check points used in accuracy assessment.

Figure 3: Javad TRIUMPH-1

As a high-precision, geodetic-grade Global Navigation Satellite System (GNSS) receiver, the TRIUMPH-1 is designed to support demanding surveying and geospatial applications that require centimeter- to millimeter-level positional accuracy [40]. Its integration into this research ensures that reference coordinates used for evaluating UAV-derived products are both reliable and traceable to established geodetic standards. The Javad TRIUMPH-1 is capable of tracking multiple GNSS constellations, including GPS, GLONASS, Galileo, and BeiDou, along with various satellite-based augmentation systems [41]. This multi-constellation tracking enhances satellite availability, improves geometric strength (low dilution of precision), and increases positioning reliability, particularly in environments where signal obstruction or multipath effects may occur. Such robustness is essential when establishing GCPs distributed across heterogeneous terrain, including open areas, near buildings, and vegetated zones within the study site. For the purposes of this research, the TRIUMPH-1 was operated using high-accuracy positioning techniques such as Real-Time Kinematic (RTK) or Post-Processed Kinematic (PPK) methods.

These techniques enable the determination of precise three-dimensional coordinates referenced to a national or global geodetic datum. The resulting GCP coordinates serve as ground truth data for constraining photogrammetric models in the "with GCP" workflow and for validating positional accuracy in the "without GCP" workflow. The high level of precision provided by the receiver ensures that any observed discrepancies in UAV mapping outputs can be attributed to differences in georeferencing strategy rather than uncertainties in ground measurements.

2.3 Ground Markers

Ground markers are artificial reference targets placed on the ground to provide clearly identifiable points in aerial imagery (Figure 4).

Figure 4: Ground markers

Their primary function is to link image-based measurements to precise real-world coordinates, thereby improving the geometric accuracy and reliability of mapping products. These markers are typically designed with high-contrast patterns, such as crosses or checkerboards, so they can be easily detected and accurately measured in multiple overlapping images. One of the most important uses of ground markers is for establishing GCPs. The coordinates of these markers are measured using high-precision GNSS surveying techniques as RTK observations [42]. During photogrammetric processing, the known coordinates are incorporated into the bundle adjustment process, which strengthens the geometric model and significantly improves both horizontal and vertical accuracy [43]. Properly distributed GCPs help reduce systematic distortions, such as tilting or warping, and ensure that orthomosaics, digital surface models (DSMs), and three-dimensional point clouds are correctly georeferenced. Ground markers are also used as independent check points for accuracy assessment. In this case, their surveyed coordinates are not included in model adjustment but are instead used to calculate positional errors, such as root mean square error (RMSE). In addition, well-distributed markers contribute to photogrammetric block stability, particularly in large or flat areas where geometric weaknesses may occur. By providing strong spatial

constraints across the study area, they improve model consistency, ensure correct scale and orientation, and enhance overall mapping reliability. Consequently, ground markers play a critical role in achieving high-precision results and validating the quality of UAV photogrammetric surveys.

2.4 Camera

For optimal photogrammetric performance, the use of ultra-wide angle and fisheye lenses should be avoided due to their significant geometric distortions, which can negatively affect camera calibration and image alignment. A focal length equivalent to approximately 50 mm (35 mm format) is generally recommended, as it provides a balanced field of view with minimal distortion [44]. In practice, lenses within the 20–80 mm focal length range (35 mm equivalent) are suitable for most mapping applications [45]. If imagery has been acquired using a fisheye lens, the correct camera sensor model must be selected in the camera calibration settings (e.g., within photogrammetric software) prior to processing to ensure accurate distortion modeling.

Fixed focal length lenses are preferred because they offer greater optical stability and more consistent calibration parameters [46]. When zoom lenses are used, the focal length should remain constant throughout the entire image acquisition session either set to the minimum or maximum value to ensure stable internal geometry. If images are captured at intermediate focal lengths, they should be assigned to separate camera calibration groups to maintain accurate processing results. Appropriate camera settings are equally important for high-quality data acquisition. Capturing images in RAW format and converting them losslessly to TIFF is recommended, as JPEG compression can introduce artifacts and noise that degrade photogrammetric accuracy [47]. The ISO setting should be kept as low as possible to minimize image noise. A sufficiently high aperture value (higher f-number) should be selected to ensure adequate depth of field and sharp image capture. Additionally, the shutter speed must be fast enough to prevent motion blur caused by platform movement or vibration, thereby preserving image clarity and feature detectability.

In this study, the DJI camera model FC330 was used. It has been widely adopted in aerial mapping and photogrammetry studies due to its balance of resolution and reliability. The FC330 integrates a 1/2.3-inch CMOS sensor that captures imagery at approximately 12.4 megapixels, with typical pixel dimensions of around 4864 × 3648 and a focal length of roughly 9 mm [48], suitable for capturing high-quality nadir photographs for orthophoto generation and 3D reconstruction at moderate flight altitudes. In UAV mapping applications, the FC330 enables sufficient ground sampling density and feature detail to support Structure-from-Motion (SfM) processing, dense point cloud generation, and digital surface model derivation when paired with appropriate flight planning and overlap parameters. Its performance has been documented in academic UAV survey campaigns where it provided reliable imagery for orthomosaic and surface model outputs. Although not as advanced as newer large-sensor or global-shutter payloads, the FC330 remains a cost-effective option in research and practice for many environmental and topographic mapping projects due to its consistent image quality and integration with common photogrammetric workflows.

2.5 Software Used

Agisoft Metashape (formerly known as Agisoft PhotoScan) is a widely used photogrammetric processing software designed for generating high-resolution 2D and 3D geospatial products from overlapping imagery acquired by UAVs. It is based on advanced Structure-from-Motion (SfM) and Multi-View Stereo (MVS) algorithms, which enable automated image alignment, camera calibration, dense point cloud generation, and surface reconstruction [13]. Due to its robust processing capabilities and compatibility with georeferenced data, Agisoft Metashape has become a standard tool in academic research and professional mapping applications. In UAV mapping workflows, the software performs a sequence of automated and semi-automated steps. Initially, it detects and matches key points across multiple overlapping images to estimate camera positions and orientations through bundle adjustment. This process generates a sparse point cloud that represents the basic geometry of the surveyed area. When Ground Control Points (GCPs) are introduced, the software integrates their surveyed coordinates into the adjustment process, thereby improving absolute positioning accuracy and minimizing geometric distortions.

Following image alignment, Agisoft Metashape generates a dense point cloud using multi-view stereo reconstruction techniques [49]. From this dense dataset, digital surface models (DSMs), and textured three-dimensional mesh models can be derived. These outputs form the basis for detailed 3D analysis, including topographic modeling, volume estimation, infrastructure inspection, and environmental assessment. The software also enables classification of point clouds and filtering of ground points for terrain extraction, enhancing the reliability of elevation-based products. For two-dimensional (2D) mapping, Agisoft Metashape produces high-resolution orthomosaics by orthorectifying and

mosaicking individual images based on the reconstructed surface model [50]. The resulting orthophotos are geometrically corrected, scale-consistent, and suitable for accurate distance, area, and spatial analysis within Geographic Information Systems (GIS). The software supports various coordinate systems and export formats, facilitating integration with other geospatial platforms.

A key advantage of Agisoft Metashape lies in its flexibility and accuracy control. Users can define processing quality levels, adjust camera calibration parameters [51], import GNSS data, and perform accuracy assessments through error statistics such as root mean square error (RMSE). This level of control makes it particularly suitable for comparative studies evaluating UAV mapping performance under different georeferencing strategies, including workflows conducted with and without Ground Control Points. Overall, Agisoft Metashape provides a comprehensive and reliable solution for transforming UAV imagery into precise 2D and 3D mapping products. Its advanced algorithms, support for georeferenced data, and adaptability to various research and engineering applications make it a critical tool in modern UAV photogrammetry [52].

2.6 Flight Planning

The flight plan was developed using the DroneDeploy application. The unmanned aerial vehicle (UAV) was assigned a flight altitude of 90 meters, with 70% sidelap and 70% overlap. The selection of 70% forward overlap and 70% sidelap is supported by established principles of image-based three-dimensional reconstruction. A 70% forward overlap ensures that consecutive images contain sufficient shared features [53], which is critical for reliable feature detection, tie point extraction, and image alignment within the Structure-from-Motion (SfM) workflow. The increased redundancy in image observations enhances the robustness of bundle adjustment, improves geometric stability, and reduces the probability of gaps or mismatches in the reconstructed model.

Similarly, a 70% sidelap between adjacent flight lines strengthens lateral connectivity within the photogrammetric block. Adequate sidelap improves the overall geometric configuration of the dataset, mitigates edge distortions, and promotes uniform coverage across the survey area. This is particularly important in environments characterized by complex topography or heterogeneous land cover, where insufficient overlap may lead to inconsistencies or localized reconstruction errors. From an operational perspective, the 70% overlap configuration represents a practical balance between data quality and efficiency. Lower overlap values may reduce flight duration and data volume but can compromise reconstruction reliability and model completeness. Conversely, higher overlap percentages substantially increase image count, processing time, and storage demands without yielding proportionate gains in accuracy for standard mapping applications. Therefore, a 70% forward overlap and 70% sidelap are widely regarded as an optimal and efficient standard for generating accurate orthomosaics and digital surface models in UAV photogrammetry [54].

The maximum flight speed for image acquisition was set at 12 m/s to maintain image quality and minimize motion blur. The total flight duration, number of images to be captured, and the required number of batteries to cover the entire study area were estimated automatically at https://www.dronedeploy.com/.

2.7 Grond Sampling Distance (GSD)

Ground Sampling Distance (GSD) is a fundamental parameter in photogrammetry and UAV-based mapping that defines the spatial resolution of an image. It represents the real-world ground distance covered by a single pixel in the captured imagery. GSD is primarily determined by the camera sensor characteristics, focal length, and flight altitude above ground level. Figure 5 illustrates the relation between camera sensor size and ground distance using similar triangle rule. The GSD is determined using Equations 1 to 3:

$$\frac{S_W}{F_R} = \frac{D_W}{H}$$

Equation 1

Where:

S_W is sensor width (mm)
F_R is the focal length of camera (mm)
H is flight altitude (mm)
D_W is the ground distance (mm)

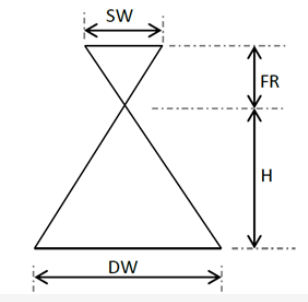

Figure 5: Relationship between camera sensor size and ground distance

The ground distance (D_W) is determined from Equation 2:

$$D_W = GSD \times \mathrm{Im}_W$$

Equation 2

Where:

Im_W is the image width (pixel)

$$GSD = \frac{S_W H}{F_R Im_W}$$

Equation 3

Accurate calculation of GSD is essential for mission planning, as it directly influences the level of detail, measurement accuracy, and suitability of the data for specific applications. Therefore, understanding and properly estimating GSD ensures that mapping objectives are achieved efficiently and with the required spatial precision.

2.8 RTK Measurement

In UAV photogrammetry, Real-Time Kinematic (RTK) is a high-precision GNSS positioning technique used to obtain centimeter-level coordinates for ground points. RTK works by using a base station placed over a known coordinate and a rover receiver that moves to different survey points [55]. The base station sends real-time correction data to the rover via radio or internet (NTRIP), correcting satellite signal errors such as atmospheric delay and orbital inaccuracies. This allows the rover to record highly accurate X, Y, and Z coordinates, which are essential for producing reliable mapping outputs such as orthomosaics, DSMs, and 3D models. To create a Ground Control Point (GCP) using RTK, a clearly visible ground target (Figure 4) is placed within the UAV survey area before the flight. The surveyor positions the RTK rover pole precisely over the center of the target as illustrates in Figure 6, ensuring it is perfectly vertical (using a bubble level), and records the corrected coordinate once the solution status shows "FIX" (indicating centimeter accuracy).

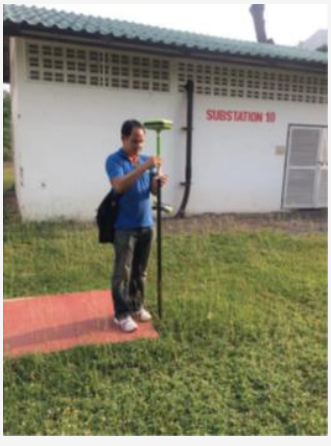

Figure 6: RTK measurement

These GCP coordinates are then imported into photogrammetry software (Agisoft Metashape) to accurately georeference and scale the UAV imagery. GCPs directly control and improve the absolute positional accuracy of the final map products [56]. A Check Point (CP) is measured using the same RTK method but is not used during model processing. Instead, CPs are reserved for independent accuracy assessment. After processing the UAV data with GCPs, the coordinates derived from the photogrammetric model are compared with the RTK-measured CP coordinates to calculate horizontal and vertical errors (RMSE). While GCPs strengthen and correct the model, CPs validate its accuracy, ensuring the final outputs meet required surveying or engineering standards.

2.9 Photogrammetric Processing

The photogrammetric processing workflow presented in Figure 7 is used to transform overlapping digital images into accurate geospatial products, including three-dimensional (3D) surface models, Digital Elevation Models (DSM), and orthomosaics. The procedure is based on structure-from-motion (SfM) and multi-view stereo (MVS) algorithms, which automatically reconstruct scene geometry from multiple photographs taken from different viewpoints. The workflow illustrated in Figure 7 outlines the sequential photogrammetric processing steps implemented in this study. Each stage of the workflow represents a critical processing component, ensuring geometric accuracy, spatial consistency, and data reliability. The individual steps of this procedure are explained in detail below.

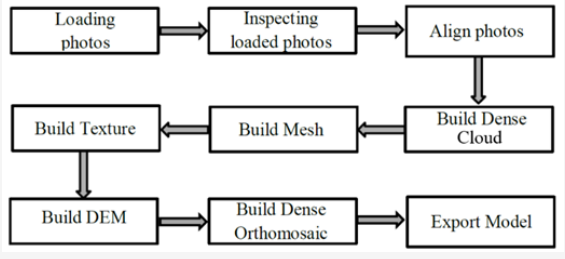

Figure 7: Orthophoto and DEM modelling in Agisoft photoscan

Stage 1: Camera Alignment

In the first stage, the software detects and matches common features across overlapping photographs. Based on these correspondences, it estimates the position and orientation of each camera and refines the camera calibration parameters. The output of this stage is a sparse point cloud and a set of estimated camera positions. The sparse point cloud represents

the initial alignment result and is not directly used in subsequent modeling processes.

Stage 2: Dense Point Cloud Generation
In the second stage, a dense point cloud is generated using the estimated camera positions and the original images. This point cloud provides a detailed representation of the object or terrain surface. Prior to further processing or export, the dense point cloud may be edited and classified to improve accuracy and remove noise.

Stage 3: Surface Reconstruction (Mesh and/or DEM Generation)
The third stage involves surface reconstruction, resulting in either a 3D polygonal mesh model and/or a Digital Elevation Model (DEM). The mesh model represents the object's surface geometry derived from the dense (or sparse) point cloud. The DEM can be generated in geographic, planar, or cylindrical coordinate systems, depending on project requirements. If the dense point cloud has been classified in the previous stage, specific point classes can be selected for DEM generation to enhance model reliability.

Stage 4: Texturing and Orthomosaic Generation
Following surface reconstruction, the mesh model can be textured to create a realistic 3D representation. Alternatively, or additionally, an orthomosaic can be produced. The orthomosaic is generated by projecting the original imagery onto a selected surface, either the DEM or the mesh model, resulting in a geometrically corrected and spatially accurate image product.

3. Results and Discussion

3.1 Geometric Accuracy

In this study, the UAV survey was conducted at a flight altitude of 96 m, resulting in a ground sampling distance (GSD) of 3.45 cm/pixel and covering a total area of 0.252 km². Based on the photogrammetric processing results, the Root Mean Square Error (RMSE) values for the GCPs and CPs were 26.26 cm and 76.76 cm, respectively. The RMSE value of 26.26 cm at the GCPs indicates the level of residual error after model adjustment and georeferencing [55]. Ideally, GCP RMSE values should approach the magnitude of the GSD (or within a few multiples of it) in well-optimized surveys [57]. In this case, the GCP RMSE corresponds to approximately 7–8 times the GSD, suggesting moderate positional discrepancies that may be attributed to factors such as GCP distribution, measurement uncertainty, image quality, or insufficient geometric strength in the block configuration [58].

More notably, the RMSE at the CPs (76.76 cm) is substantially higher than that of the GCPs. Since CPs serve as independent accuracy validators and are not included in the model adjustment, their RMSE provides a more realistic assessment of the overall geospatial accuracy of the orthomosaic. The CP error is approximately three times larger than the GCP error and more than twenty times the GSD, indicating a significant reduction in external accuracy [59]. This discrepancy suggests potential issues such as uneven GCP placement, edge effects within the study area, systematic distortions, or weaknesses in the elevation model used for orthorectification. Overall, while the project achieved centimeter-level image resolution, the decimeter- to sub-meter-level RMSE values indicate that the final orthophoto accuracy does not fully match the theoretical precision implied by the GSD. Therefore, improvements in GCP distribution, survey methodology, and network geometry would likely be necessary to enhance positional reliability in future surveys.

3.2 Orthophoto Comparison

The comparison of the orthophoto maps generated using the UAV mapping technique, with and without GCPs, is presented in Figure 8. This comparison highlights the influence of GCP integration on geometric consistency, and overall map quality. By examining both outputs side by side, the differences in spatial alignment and distortion can be clearly observed. According to Figure 8, the orthophoto processed without GCPs demonstrates comparatively better visual quality and structural consistency (Figure 8(a)). In contrast, the orthophoto generated with GCPs integration exhibits noticeable distortions. Several buildings appear deformed and do not retain their true polygonal shapes as observed in reality (Figure 8(b)). An orthomosaic generated from UAV imagery using GCPs may sometimes appear more distorted, particularly around buildings and other vertical structures because the processing software is constrained to align the imagery with precise, survey-grade ground coordinates. This georeferencing constraint improves absolute positional accuracy; however, it can also reveal geometric inconsistencies that were previously masked in unconstrained models.

In contrast, the integration of GCPs imposes rigid spatial constraints during bundle adjustment. While this improves absolute horizontal and vertical positioning, it may simultaneously reveal underlying systematic distortions that were previously masked in the free-network solution [60].

Figure 8: Comparison of orthophoto map: (a) with GCPs, and (b) without GCPs

The observed deformation of building geometries in the GCP-constrained orthomosaic likely reflects the correction of accumulated internal block errors, camera calibration instability, or uneven GCP spatial distribution.

Several factors explain why the integration of GCPs can make buildings appear more distorted:

Correction of Rubber-Sheeting Effects:
Without GCPs, the software may distribute geometric errors across the model, effectively "stretching" or "warping" the orthomosaic to achieve a visually coherent result. When GCPs are introduced, the model becomes rigidly constrained to match known ground coordinates [61]. Consequently, vertical structures such as buildings may appear twisted or warped as the system corrects previously distributed distortions.

Correction of Camera Tilt and Perspective:
GCPs refine the absolute orientation of the imagery. If the UAV flight included camera tilt, oblique viewing angles, or lens distortion, the adjustment process may accentuate perspective-related deformations, such as building lean. These effects are not newly introduced errors but rather corrections that expose the true geometric relationships within the dataset [62].

Doming Effect Compensation:
UAV-derived models processed without sufficient ground control often exhibit a systematic "doming" or "bowl" effect, where the center of the model is

vertically biased relative to the edges [63]. The incorporation of GCPs corrects this systematic error. However, if GCP distribution is inadequate particularly in areas with significant elevation variation, the correction may result in localized distortions, especially along building façades [64].

Elevation and DSM-Related Influences:
Orthophotos are generated by projecting a three-dimensional surface model (DSM) onto a two-dimensional plane. Apparent distortions in buildings may therefore reflect limitations or inconsistencies in the elevation model rather than errors in the orthorectification process itself. In summary, orthomosaics generated without GCPs may appear visually smoother but typically exhibit lower absolute accuracy, often within the meter-level range. Conversely, GCP-constrained models achieve higher positional accuracy, frequently at the centimeter level, while potentially revealing geometric distortions that were previously concealed [65]. To reduce distortion effects in GCP-based processing, it is recommended to (1) increase the number of well-distributed GCPs, particularly around project boundaries and in areas with significant height variation; (2) incorporate independent checkpoints to verify positional accuracy; and (3) ensure that GCPs are placed on stable, flat ground surfaces rather than on sloped terrain or near vertical obstacles.

3.3 Digital Surface Model (DSM) Analysis
The DSMs generated from processing with and without GCPs exhibit generally similar shapes and overall surface characteristics. However, the DSM produced without GCPs appears to contain slightly more visible detail compared to the GCP-constrained model. Despite this minor variation, the difference is not readily distinguishable to the naked eye at normal viewing scale and becomes apparent only upon closer inspection or magnification, as illustrated in Figure 9. The vertical accuracy of DSM derived from UAV photogrammetry differ substantially depending on whether GCPs are incorporated. Although DSM generated without GCPs may adequately represent the relative morphology of the terrain, they commonly exhibit significant systematic vertical errors. These errors often manifest as tilting or "doming" (bowing) effects, resulting in reduced absolute elevation accuracy compared with models constructed using GCPs.

(a) (b)

Figure 9: Comparison of DSM results: (a) with GCPs, and (b) without GCPs

Several key distinctions characterize DSM produced with and without GCPs. First, in terms of absolute accuracy, GCP-integrated models typically achieve high vertical precision, frequently within the centimeter range under appropriate survey conditions. In contrast, DSM generated without GCPs may exhibit substantially larger vertical discrepancies, in some cases reaching several meters. Second, UAV-based mapping conducted without GCPs or high-precision positioning systems (e.g., RTK/PPK GNSS) is particularly susceptible to systematic distortions, including doming effects in which the central portion of the model is vertically offset relative to its margins. Third, while non-GCP models may preserve relative topographic relationships such as the elevation difference between a hill and an adjacent valley, they often fail to provide reliable absolute elevations referenced to a geodetic datum.

GCPs play a critical role in constraining photogrammetric models to real-world coordinate systems, thereby minimizing geometric distortions and improving overall vertical and horizontal accuracy. In summary, the integration of GCPs is essential for producing accurate, georeferenced DSM suitable for applications requiring high absolute vertical precision [66]. Conversely, DSM generated without GCPs may be adequate only for analyses focused on relative topographic variation where absolute elevation accuracy is not a primary requirement. From a practical perspective, the results emphasize that the choice between GCP-supported and non-GCP workflows must be application-driven. For projects requiring only relative measurements, such as qualitative terrain visualization or preliminary site assessment, non-GCP processing may be operationally efficient. However, for engineering design, cadastral mapping, volumetric computation, or infrastructure monitoring, the integration of well-distributed GCPs remains indispensable.

4. Conclusion

This study presented a comprehensive comparative evaluation of UAV photogrammetric mapping performed with and without the integration of GCPs, with the objective of quantifying differences in, orthophoto quality, and DSM reliability. The comparison of orthophotos illustrates the trade-off between visual smoothness and geometric correctness. The model processed without GCPs appeared visually coherent and structurally smooth because the photogrammetric solution optimized internal image alignment without rigid external constraints. However, this “free-network” configuration inherently distributes systematic errors across the block, potentially masking distortions such as global shifts or vertical bias. When GCPs were introduced, the model became rigidly anchored to real-world coordinates, exposing geometric inconsistencies that were previously concealed. Apparent building deformation in the GCP-based orthomosaic is therefore not necessarily an introduced error, but rather a manifestation of corrected systematic distortions within the unconstrained solution.

The DSM comparison reinforces these conclusions. While both DSMs preserved general terrain morphology, the non-GCP model remains susceptible to vertical bias and doming effects, which compromise absolute elevation accuracy. In contrast, the GCP-integrated DSM demonstrated improved vertical referencing, making it more suitable for engineering, volumetric analysis, and applications requiring datum-consistent elevation data. These findings confirm that relative topographic representation may be achievable without ground control, but reliable absolute positioning requires external constraints. From an operational perspective, this study underscores that the selection of a UAV mapping workflow should be guided by project requirements rather than convenience or visual appearance of outputs. For applications involving qualitative visualization or relative change detection, a non-GCP workflow may provide acceptable results with reduced field effort. However, for survey-grade mapping, infrastructure planning, cadastral applications, or any task demanding centimeter- to decimeter-level accuracy, the integration of well-distributed and accurately surveyed GCPs remains essential. In conclusion, the results affirm that GCPs continue to play a fundamental role in ensuring positional reliability in UAV photogrammetry. While technological advancements in onboard GNSS positioning are reducing dependency on extensive ground control, this study demonstrates that external validation and geometric constraints remain critical for achieving dependable and defensible geospatial products.

References

[1] Aminigbo, L., Brown, J. and Ede, P., (2022). Geospatial Data Acquisition Using Unmanned Aerial Systems (Uas): A Paradigm for Mapping the Built Environment of the Niger Delta Region of Nigeria. *International Journal of Environmental Science & Sustainable Development*, Vol. 30(7). https://doi.org/10.21625/essd.v7i2.849.

[2] Nex, F., Stathopoulou, E. K., Remondino, F., Yang, M. Y., Madhuanand, L., Yogender, Y., Alsadik, B., Weimann, M., Jutzi, B. and Qin, R., (2024). UseGeo - A UAV-Based Multi-Sensor Dataset for Geospatial Research. *ISPRS Open Journal of Photogrammetry and Remote Sensing*, Vol. 13. https://doi.org/10.1016/j.ophoto.2024.100070.

[3] Simeonova, G., Antova, G. and Mickrenska, C., (2024). Collecting Spatial Data with Unmanned AerialVehicle. *Inżynieria Mineralna*, Vol. 23. https://doi.org/10.29227/IM-2024-01-26.

[4] Sangsrichan, K., Manopkawee, P. and Kanthata, S., (2023). 3D Digital Outcrop Model for Geological Structure Analysis in Mae Moh Coal Mine, Lampang Province, Thailand. *International Journal of Geoinformatics*, Vol. 19(9); 32-43. https://doi.org/10.52939/ijg.v19i9.2847.

[5] Suhaizad, L., Khalid, N. and Abu Sari, M., (2023). Tree Height and Crown Extraction from UAV-Based Multispectral Imagery. *International Journal of Geoinformatics*, Vol. 19(5); 61-68. https://doi.org/10.52939/ijg.v19i5.2661.

[6] Phonphan, W., Arunplod, C., Niemmanee, T., Wongsongja, N., Worachairungreung, M., Kulpanich, N., and Suwattano, O., (2024). Integration of Drone-based Imaging for Coastal Ecosystem Mapping: A Case Study of Shallow Coastal in Phang Nga Bay, Thailand. *International Journal of Geoinformatics*, Vol. 21(1); 121–144. https://doi.org/10.52939/ijg.v21i1.3801.

[7] Chonpatathip, S., (2023). Earthwork Volume Measurement in Road Construction Using Unmanned Aerial Vehicle (UAV). *International Journal of Geoinformatics*, Vol. 19(12); 51–64. https://doi.org/10.52939/ijg.v19i12.2977.

[8] Chonpatathip, S., Suanpaga, W. and Chantawarangul, K., (2023). Utilizing Unmanned Aerial Vehicles (UAVs) for Earthwork Fill Height Determination in Road Construction. *International Journal of Geoinformatics*, Vol. 19(10); 28–39. https://doi.org/10.52939/ijg.v19i9.2877.

[9] Chathuranga, M., Darwin, N., Ahmad, A., Sandamali, J. and Gohari A., (2025). Trends, Advancements, and Future Directions of Unmanned Aerial Vehicle Technology-Based Stockpile Volume Estimation: A Systematic Review. *International Journal of Geoinformatics*, Vol. 21(11); 94-120. https://doi.org/10.52939/ijg.v21i11.4605.

[10] Ibrahim, A., Afonja, Y. O., Omale, D., Idoko, I. A., Alagbe, A. O., Oduyemi, A. T., Akintuyi, B., Akintuyi, O. B., Ibrahim, R. O. and Azeez, Z. O., (2025). Assessment of Unmanned Aerial Vehicle Versus Terrestrial Method of Topographic Surveying. *Environmental Technology and Science Journal*, Vol. 19(16); 89–101. https://doi.org/10.4314/etsj.v16i1.9.

[11] Sestras, P., Badea, G., Badea, A. C., Salagean, T., Roșca, S., Kader, S. and Remondino, F., (2025). Land Surveying with UAV Photogrammetry and Lidar for Optimal Building Planning. *Automation in Construction*, Vol. 173. https://doi.org/10.1016/j.autcon.2025.106092.

[12] Cahyadi, M. N., Asfihani, T., Suhandri, H. F. and Navisa, S. C., (2023). Analysis of GNSS/IMU Sensor Fusion at UAV Quadrotor for Navigation. *Earth and Environmental Science*, Vol. 1276. https://doi.org/10.1088/1755-1315/1276/1/012021.

[13] Kholil, M., Ismanto, I. and Fu'ad, M. N., (2021). 3D Reconstruction using Structure from Motion (SFM) Algorithm and Multi View Stereo (MVS) Based on Computer Vision. *IOP Conference Series Materials Science and Engineering,* Vol. 103(1). https://doi.org/10.1088 /1757-899X/1073/1/012066.

[14] Luong, N., Tran, D. C. and Doung, C., (2023). Applying GIS and Geospatial Measurement Technologies in Construction Data Management in Vietnam: A Case Study of Hanoi University of Civil Engineering's Campus. *International Journal of Geoinformatics*, Vol. 19(10); 40–50. https://doi.org/10.52939/ijg.v19i9.2879.

[15] [15] Thanh, P., Elshewy, M., Long, N. and Thom, T., (2032). Creation and Assessment of a Topographic Map from Unmanned Aerial Vehicle Data in Thanh Son District, Vietnam. *International Journal of Geoinformatics*, Vol. 19(3); 57–66. https://doi.org/10.52939/ijg.v19i3.2605.

[16] Srinoi, T., Bannakulpiphat, T., Santitamnont, P. and Vaiphasa, C., (2024). Building Height Estimation from Open Optical Remote Sensing by Machine Learning Regression Technique: A Case Study of the Central of Bangkok. *International Journal of Geoinformatics*, Vol. 20(9); 20(9):43–53. https://doi.org/10.52939/ijg.v20i9.3543.

[17] On, C., Kanniah, K. and Lau, A., (2024). A Multiscale Quantification of Leaf Area Index with Unmanned Aerial Vehicle and SPOT-7 Satellite Imageries: A case of Kuala Lumpur, Malaysia. *International Journal of*

Geoinformatics, Vol. 20(5); 54–68. https://doi.org/10.52939/ijg.v20i5.3231.

[18] Chetverikov, B., Trevoho, I., Prokhorchuk, O., Vladimirov, S. and Herasymchuk, P., (2024). Synergy of UAV Aerial Survey Methods and LiDAR Scanning for the Study of Planar Objects of Historical and Cultural Heritage. *International Journal of Geoinformatics*, Vol. 20(9); 98–111. https://doi.org/10.52939/ijg.v20i9.3551.

[19] Shukri, S., Asmat, A., Rahiman, M., Japeiri, A. and Sahwee, Z., (2024). Real-time Vertical Air Quality Monitoring System Development for Urban Scale. *International Journal of Geoinformatics*, Vol. 20(8); 102–14. https://doi.org/10.52939/ijg.v20i8.3463.

[20] Bashit, N., Sasmito, B., Maladzi, H., Haryadi, S., Parsetyo, Y. and Yuwono, B., (2025). Analysis of River Flow Velocity Measurement Using the Large Scale Particle Image Velocimetry Method. *International Journal of Geoinformatics*, Vol. 21(9); 102–19. https://doi.org/10.52939/ijg.v21i9.4449.

[21] Kulpanich, N., Worachairungreung, M., Thanakunwutthirot, K. and Chaiboonrueang, P., (2023). The Application of Unmanned Aerial Vehicles (UAVs) and Extreme Gradient Boosting (XGBoost) to Crop Yield Estimation: A Case Study of Don Tum District, Nakhon Pathom, Thailand. *International Journal of Geoinformatics*, Vol. 19(2); 65–77. https://doi.org/10.52939/ijg.v19i2.2569.

[22] Kedys, J., Tchappi, I. and Najjar, A., (2024). UAVs for Disaster Management - An Exploratory Review. *Procedia Computer Science*, Vol. 231; 129–136. https://doi.org/10.1016/j.procs.2023.12.184.

[23] Alawad, W., Halima, N. and Ben A. L., (2023). An Unmanned Aerial Vehicle (UAV) System for Disaster and Crisis Management in Smart Cities. *Electronics (Basel),* Vol. 12(4). https://doi.org/10.3390/electronics12041051.

[24] Nikhil, N., Shreyas, S. M., Vyshnavi, G. and Yadav, S., (2020). Unmanned Aerial Vehicles (UAV) in Disaster Management Applications. *2020 Third International Conference on Smart Systems and Inventive Technology (ICSSIT)*, 140–148. https://doi.org/10.1109/ICSSIT48917.2020.9214241.

[25] Benito, C. and Opon, J., (2024). Impact of Varying Ground Control Points Configurations on the Accuracy of Unmanned Aerial Vehicle-Based Digital Elevation Models. *International Journal of Geoinformatics*, Vol. 20(11); 134–147. https://doi.org/10.52939/ijg.v20i11.3705.

[26] Urban, R., Štroner, M. and Kuric, I., (2020). The use of Onboard UAV GNSS Navigation Data for Area and Volume Calculation. *Acta Montanistica Slovaca*, Vol. 1(2); 361–374. https://doi.org/10.46544/AMS.v25i3.9.

[27] Zhou, J., He, L. and Luo, H., (2023). Real-Time Positioning Method for UAVs in Complex Structural Health Monitoring Scenarios, *Drones*. Vol. 7(3). https://doi.org/10.3390/drones7030212.

[28] Seo, D. M., Woo, H. J., Hong, W. H., Seo, H. and Na W. J., (2024). Optimization of Number of GCPs and Placement Strategy for UAV-Based Orthophoto Production. *Applied Sciences*, Vol. 14(8). https://doi.org/10.3390/app14083163.

[29] Zhong, H., Duan, Y., Tao, P. and Zhang, Z., (2025). Influence of Ground Control Point Reliability and Distribution on UAV Photogrammetric 3D Mapping Accuracy. *Geo-spatial Information Science*, Vol. 28(5); 1998–2018. https://doi.org/10.1080/10095020.2025.2451204.

[30] Syetiawan, A., Maharani, M., Nugroho, A., Setyo, R., Apriyanti, D., Augustian, M., and Prihantin, S. M., (2025). Precise 3d Modelling Using Combination Depth Maps Processing and Ground Control Point. *International Journal of Geoinformatics*, Vol. 21(4); 71–81. https://doi.org/10.52939/ijg.v21i4.4079.

[31] Teppati Losè, L., Chiabrando, F., and Giulio Tonolo, F., (2020). Boosting the Timeliness of UAV Large Scale Mapping. Direct Georeferencing Approaches: Operational Strategies and Best Practices. *ISPRS International Journal of Geo-Information*, Vol. 9(10). https://doi.org/10.3390/ijgi9100578.

[32] Martínez-Carricondo, P., Agüera-Vega, F., and Carvajal-Ramírez, F., (2023). Accuracy Assessment of RTK/PPK UAV-Photogrammetry Projects using Differential Corrections from Multiple GNSS Fixed Base Stations. *Geocarto International*, Vol. 38(1). https://doi.org/10.1080/10106049.2023.2197507.

[33] Rehak, M. and Skaloud, J., (2017). Time Synchronization of Consumer Cameras on Micro Aerial Vehicles. *ISPRS Journal of Photogrammetry and Remote Sensing,* Vol. 31(123); 114–23. https://doi.org/10.1016/j.isprsjprs.2016.11.009.

[34] Thammaboribal, P., Tripathi, N. and Lipiloet, S., (2024). Pre-Seismic Signature Detection using Diurnal GPS-TEC and Kriging Interpolation Maps (ASK-VTEC Technique): 11 May 2011, M9.0 Tohoku Earthquake Case

Study. *International Journal of Geoinformatics*, Vol. 20(11); 148–161. https://doi.org/10.52939/ijg.v20i11.3715.

[35] Cho, J., Jeong, S. and Lee, B., (2026). Optimal Ground Control Point Layout for UAV Photogrammetry in High Precision 3D Mapping. *Measurement*, Vol. 257. https://doi.org/10.1016/j.measurement.2025.118343.

[36] Türk Phd, T., Bahadur, B., Demirel, Y., Altuntas, C. and Ocalan, T., (2025). Investigation of the Effect of GCP Number and Distribution on Photogrammetric Product Accuracy in UAV Photogrammetry. *Journal of Geodesy and Geoinformation*, Vol. 12; 77–88. https://doi.org/10.9733/JGG.2025R0006.E.

[37] Silva, M., Eger, R., Rosenfeldt, Y. and Loch, C., (2018). Testing Dji Phantom 4 Pro for Urban Georeferencing. *ISPRS - International Archives of the Photogrammetry, Remote Sensing and Spatial Information Sciences*, Vol. XLII-1; 407-411. https://doi.org/10.5194/isprs-archives-XLII-1-407-2018.

[38] Peppa, M. V., Hall, J., Goodyear, J. and Mills, J., (2019). Photogrammetric Assessment and Comparison of Dji Phantom 4 Pro and Phantom 4 Rtk Small Unmanned Aircraft Systems. *ISPRS - International Archives of the Photogrammetry, Remote Sensing and Spatial Information Sciences*, Vol. XLII-2(W13); 503–509. https://doi.org/10.5194/isprs-archives-XLII-2-W13-503-2019.

[39] Garwood, B., (2018). Review: DJI Phantom 4 Pro+ Drone Is an Easy Addition to Campus Fleet. [Online]. Available: https://edtechmagazine.com/higher/article/2018/12/review-dji-phantom-4-pro-drone-easy-addition-campus-fleet. [Accessed: Feb. 11, 2026].

[40] Murgia, F., Mitache, A., Rehak, M., Strecha, C., and Vidmar, B., (2021). Investigation on the Positional Accuracy of 3D Models Generated by the Pix4Dcatch App Synchronized with the viDoc RTK Rover for iPad.

[41] Javad. (n.d.), TRIUMPH-1M GNSS Smart Antenna. [Online]. Available: https://www.javad.com/wp-content/uploads/TRIUMPH-1M_Datasheet_white_2page_v1_10.16.22.pdf. [Accessed: Feb. 14, 2026].

[42] Alkan, M., (2024). High-Precision UAV Photogrammetry with RTK GNSS: Eliminating Ground Control Points. Hittite *Journal of Science and Engineering*, Vol. 31(1); 139–147. https://doi.org/10.17350/HJSE19030000341.

[43] Xing, L., Li, Y. and Yue, C., (2025). Improvement of UAV-Photogrammetric Survey Accuracy Using Point Feature Constraints of Markers. *Journal of the Indian Society of Remote Sensing*, Vol. 53(12); 4421–4433. https://doi.org/10.1007/s12524-025-02246-4.

[44] Gbopa, A., Ayodele, E., Okolie, C., Ajayi, A. and Iheaturu, C., (2021). Unmanned Aerial Vehicles for Three dimensional Mapping and Change Detection Analysis. *Geomatics and Environmental Engineering*, Vol. 15(1); 41–61. https://doi.org/10.7494/geom.2021.15.1.41.

[45] Roncella, R. and Forlani, G., (2021). UAV Block Geometry Design and Camera Calibration: A Simulation Study. *Sensors*, Vol. 21(18). https://doi.org/10.3390/s21186090.

[46] Maes, W. H., (2025). Practical Guidelines for Performing UAV Mapping Flights with Snapshot Sensors. *Remote Sensing,* Vol. 17(4). https://doi.org/10.3390/rs17040606.

[47] Wu, Z., Wang, X., Jia, M., Liu, M., Sun, C., Wu, C. and Wang, J., (2024). Dense Object Detection Methods in RAW UAV Imagery Based on YOLOv8. *Scientific Reports*, Vol. 14(1). https://doi.org/10.1038/s41598-024-69106-y.

[48] Kovanič, Ľ., Topitzer, B., Peťovský, P., Blišťan, P., Gergeľová, M. B. and Blišťanová, M., (2023). Review of Photogrammetric and Lidar Applications of UAV. *Applied Sciences*, Vol. 13(11). https://doi.org/10.3390/app13116732.

[49] Asadpour, A., (2021). Documenting Historic Tileworks Using Smartphone-based Photogrammetry. *Mersin Photogrammetry Journal*, Vol. 3(1); 15–20. https://doi.org/10.53093/mephoj.899432.

[50] Peterson, J., Li, W., Cesar-Tondreau, B., Bird, J., Kochersberger, K., Czaja, W. and McLean, M., (2019). Experiments in Unmanned Aerial Vehicle/Unmanned Ground Vehicle Radiation Search. *Journal of Field Robotics*, Vol. 36(4); 818–845. https://doi.org/10.1002/rob.21867.

[51] Rahman, A. D. M. B. and Cahyono, A., (2023). Analysis Of 3-D Building Modeling Using Photogrammetric Software: Agisoft Metashape and Micmac. *IOP Conference Series: Earth and Environmental Science*, Vol. 1276. https://doi.org/10.1088/1755-1315/1276/1/012044.

[52] Jarahizadeh, S. and Salehi, B., (2024). A Comparative Analysis of UAV Photogrammetric Software Performance for Forest 3D Modeling: A Case Study Using AgiSoft Photoscan, PIX4DMapper, and DJI Terra. *Sensors*, Vol. 24(1). https://doi.org/10.3390/s24010286.

[53] Lemus-Romani, J., Rueda, E. J., Becerra-Rozas, M., Cabrera, C., Liu, J. and Astorga, G., (2025). Optimization of UAV Flight Parameters for Urban Photogrammetric Surveys: Balancing Orthomosaic Visual Quality and Operational Efficiency. *Drones*. Vol. 9(11). https://doi.org/10.3390/drones9110753.

[54] Yang, Z., Hu, K., Kou, W., Xu, W., Wang, H. and Lu, N., (2025). Enhanced Recognition and Counting of High-Coverage Amorphophallus Konjac by Integrating UAV RGB Imagery and Deep Learning. *Scientific Reports*. Vol. 15(1). https://doi.org/10.1038/s41598-025-91364-7.

[55] Ekaso, D., Nex, F. and Kerle, N., (2020). Accuracy Assessment of Real-Time Kinematics (RTK) Measurements on Unmanned Aerial Vehicles (UAV) for Direct Geo-Referencing. *Geo-spatial Information Science*. Vol. 23(2); 165–181. https://doi.org/10.1080/10095020.2019.1710437.

[56] Pilarska-Mazurek, M., and Łoza, D., (2025). Analysis of the Influence of RTK Observations on the Accuracy of UAV Images. *Applied Sciences*. Vol. 15(19). https://doi.org/10.3390/app151910559.

[57] Phojaem, T., Dangbut, A., Wisutwattanasak, P., Janhuaton, T., Champahom, T., Ratanavaraha, V. and Jomnonkwao, S., (2025). Evaluating UAV Flight Parameters for High-Accuracy in Road Accident Scene Documentation: A Planimetric Assessment Under Simulated Roadway Conditions. *ISPRS International Journal of Geo-Information*, Vol. 14(9). https://doi.org/10.3390/ijgi14090357.

[58] Jiménez-Jiménez, S. I., Ojeda-Bustamante, W., Marcial-Pablo, M. de J. and Enciso, J., (2021). Digital Terrain Models Generated with Low-Cost UAV Photogrammetry: Methodology and Accuracy. *ISPRS International Journal of Geo-Information*, Vol. 10(5). https://doi.org/10.3390/ijgi10050285.

[59] Darwin, N., Ahmad, A. and Zainon, O., (2014). The Potential of Unmanned Aerial Vehicle for Large Scale Mapping of Coastal Area. *IOP Conference Series: Earth and Environmental Science*. Vol. 18(1). https://doi.org/10.1088/1755-1315/18/1/012031.

[60] Liu, X., Lian, X., Yang, W., Wang, F., Han, Y. and Zhang, Y., (2022). Accuracy Assessment of a UAV Direct Georeferencing Method and Impact of the Configuration of Ground Control Points. *Drones,* Vol. 6(2). https://doi.org/10.3390/drones6020030.

[61] Wang, Z., Shi, L., Li, J., Dai, W., Lu, W. and Li, M., (2025). The Synergistic Effects of GCPs and Camera Calibration Models on UAV-SfM Photogrammetry. *Drones*, Vol. 9(5). https://doi.org/10.3390/drones9050343.

[62] Chen, W. and Zhang, J., (2020). Research on 3D Modelling Based on UAV Tilt Photogrammetry with KQCAM5 Swing Tilt Camera. *Journal of Physics: Conference Series*, Vol. 1650(3). https://doi.org/10.1088/1742-6596/1650/3/032156.

[63] Mazzoleni, M., Paron, P., Reali, A., Juizo, D., Manane, J. and Brandimarte, L., (2020). Testing UAV-Derived Topography for Hydraulic Modelling in a Tropical Environment. *Natural Hazard,* Vol. 103(1); 139–63. https://doi.org/10.1007/s11069-020-03963-4.

[64] Obanawa, H., Hayakawa, Y. and Sakanoue, S., (2022). Methods to Reduce the Doming Effect of Three-Dimensional Model without GCPs in RTK-UAV Surveys. *Systems Agriculture*, Vol. 37; 29–38. https://doi.org/10.14962/jass.37.2_29.

[65] Llabani, A. and Abazaj, F., (2024). Evaluating UAV RTK Photogrammetry Mapping Accuracy in Urban Areas without Ground Control Points. *International Research Journal of Innovations in Engineering & Technology.* Vol. 8(2); 82–87. https://doi.org/10.47001/IRJIET/2024.802012.

[66] Yang, H., Li, H., Gong, Z., Dai, W. and Lu, S., (2020). Relations between the Number of GCPs and Accuracy of UAV Photogrammetry in the Foreshore of the Sandy Beach. *Journal of Coastal Research*, Vol. 95; 1372-1376. https://doi.org/10.2112/SI95-263.1.